Journal of the Korean Ceramic Society
Vol. 40, No. 4, pp. 328~332, 2003.

The Microstructure and Microwave Dielectric Properties of Ceramics in the System $CaTiO_3$-$Li_{0.5}Nd_{0.5}TiO_3$

Tristan Lowe, Feridoon Azough, and Robert Freer†

Materials Science Centre, University of Manchester / UMIST Manchester, M1 7HS, UK
(Received March 19, 2003; Accepted March 29, 2003)

ABSTRACT

Ceramics of $xCaTiO_3$-$(1-x)Li_{0.5}Nd_{0.5}TiO_3$ (xCT-(1-x)LNT) series have been prepared by the mixed oxide route. Powders were calcined at 1100°C; cylindrical specimens were fired at temperatures in the range 1300–1500°C. Sintered products were typically 90–95% dense. The microstructures were dominated by angular grains typically 1.3 μm to 3.5 μm in size. Twinning in the microstructures was analysed using Electron Back Scattered Diffraction (EBSD). Microwave dielectric properties of xCT-(1-x)LNT at 2.1 GHz (ε_r, Q×f, and τ_f) were 170, 3800 GHz and 744 ppm/°C for pure $CaTiO_3$ and 80, 2000 GHz and −240 ppm/°C for LNT. The τ_f decreases almost linearly from 744 for pure $CaTiO_3$ to −240 for pure LNT.

Key words : Perovskite, $CaTiO_3$, Microwave dielectric, Electron Back Scatter Diffraction (EBSD)

1. Introduction

The growth of the telecommunications industry over the last 15 years[1] has resulted in an increasing demand for the miniaturization of microwave components. Miniaturization can be achieved by increasing the relative permittivity (ε_r) since the size of microwave components is inversely proportional to the square root of the relative permittivity. Additional requirements are that the dielectric Q value is maximized (i.e. the dielectric losses are minimized) and the dielectric properties are temperature stable such that the temperature coefficient of resonant frequency (τ_f) is maintained close to zero (±5 ppm/°C). In some cases, materials that have similar crystal structures but opposite temperature coefficients of resonant frequency, can be combined to produce a ceramic with the desired microwave properties and zero τ_f.

During the last ten years, low loss ceramics in the system $CaTiO_3$-$Li_xLn_{1-x}TiO_3$ (Ln=Sm, Nd) have attracted much interest[2-5] because of their high relative permittivity. The calcium end member $CaTiO_3$ has ε_r of 170 and Q×f value of 2000 GHz whilst $Li_xSm_{1-x}TiO_3$ has ε_r=80 and Q×f=2100 GHz. The τ_f values of the two end members are non-zero, but of opposite polarity. Kim and Yoon[2] showed that good dielectric properties could be obtained in the system $CaTiO_3$-$Li_{0.5-3x}Sm_{0.5-x}TiO_3$ (CT-LST). However, Takahashi *et al.*[6] demonstrated that the microwave dielectric properties in such systems vary with ionic size, so that replacing Sm with Nd (increase in ionic radii) should yield a ceramic with a higher relative permittivity. Therefore in the present study, the system $xCaTiO_3$-$(1-x)Li_{0.5}Nd_{0.5}TiO_3$ has been investigated. The system (and compounds) will be abbreviated as xCT-(1-x)LNT. Near zero τ_f material should be achieved between x=0.2 and 0.4 for xCT-(1-x)LNT.[3] Pure $CaTiO_3$ exhibits a high degree of twinning within the microstructure. Petzelt and N. Setter[7] predict that since twins are a form of extrinsic defect within the structure that they will lead to an increase in microwave losses. In the present investigation of the properties of the xCT-(1-x)LNT series the morphology of twinning has also been studied.

2. Experimental Procedures

Ceramics of 0.4CT-0.6LNT were prepared by the mixed oxide route using $CaTiO_3$ (99%-ALFA AESAR), Li_2CO_3 (99%-Fluka), Nd_2O_3 (99%-Honeywell Electronic Materials) and TiO_2 (98.5%-Tioxide UK Ltd). The powders were mixed in the appropriate amounts for each composition, wet milled in propan-2-ol for 16 h, and then calcined at 1100°C for 4 h. Undoped LNT and $CaTiO_3$ were calcined at 900°C and 1250°C for 4~5 h, respectively. After calcining the powders were ball milled for a further 16 h. After drying, cylindrical samples were pressed at 50–100 MPa. In order to minimise lithium loss during firing, the specimens were surrounded in powder of the same composition and supported on a powder-covered alumina substrate. Sintering was performed in air at temperatures in the range of 1300°C and 1500°C for 3 h. The heating and cooling rates were 360°C/h and 240°C/h respectively. Product densities were determined from weight and dimension measurements.

Prior to X-ray diffraction analysis, specimens were ground using 1200 grade SiC. X-ray diffraction was undertaken using a Philips XPERT system (PW 3710) over the 2θ range

†Corresponding author : Robert Freer
E-mail : robert.freer@umist.ac.uk
Tel : +44(0)161-200-3564 Fax : +44(0)161-200-8877

10° to 100° with a step size of 0.04°. Lattice parameters were determined using CELLREF software. For micro-structural analysis all specimens were ground on 1200 grade SiC and then successively polished on 6 μm, 1 μm and 0.25 μm diamond paste followed by OPS (colloidal Silica suspension) for 5 h. The samples were investigated in detail by scanning electron microscopy (Philips SEM525 equipped with an EDAX DX4 system). Additional studies were carried out under Electron Backscatter Diffraction (EBSD) conditions using a Philips XL30 FEG SEM. Charging of the sample surface during EBSD was prevented by applying a thin carbon layer that was overlain by a mesh network of metallic silver. The EBSD maps were analysed using the hkl Channel Five software to produce orientation maps. Microwave dielectric properties were determined at 2.1 GHz by the Hakki and Coleman[8] method. The temperature coefficient of resonant frequency (τ_f) was determined by a cavity method between 20° and +60°C.

3. Results and Discussion

Fig. 1 shows the variation of density as a function of composition and sintering temperature. Products are 90 to 95% dense, which is comparable with densities of CT-LST reported by Kim and Yoon.[3] As the amount of LNT added to CT is increased the specimen density increases linearly (Fig. 1). The densities of CT and LNT are 3.85 and 4.9 gcm^{-3}, respectively. The increase in density can be attributed to

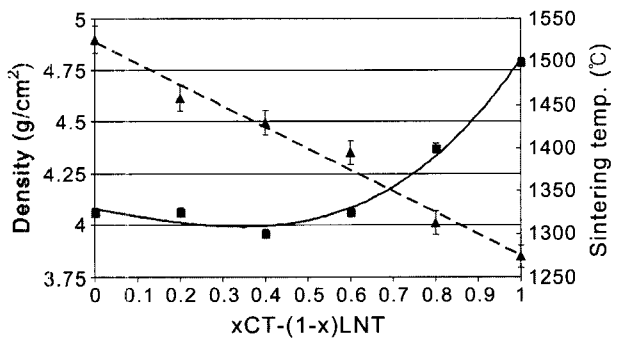

Fig. 1. Sintering temperature (■) and density (▲) as a function of composition xCT-(1-x)LNT.

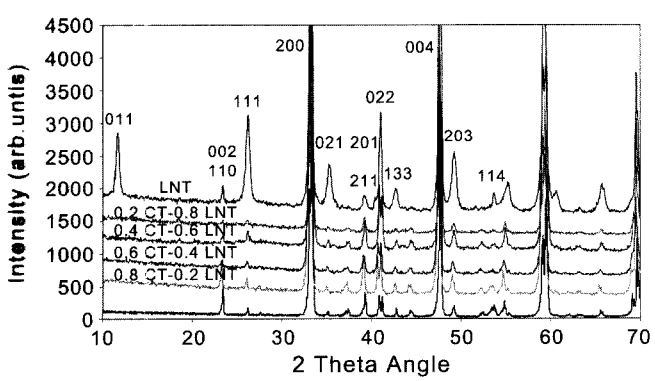

Fig. 2. XRD spectra for xCT-(1-x)LNT.

the incorporation of Nd into the $CaTiO_3$ structure. As the Li-bearing component LNT increases in the system xCT-(1-x) LNT, the sintering temperature decreases from 1500 to 1325°C. The system exhibits a minimum sintering temperature of 1325°C for 0.4CT-0.6LNT; further addition of LNT has no effect upon the sintering temperature. Fig. 2 shows XRD spectra for the xCT-(1-x)LNT. It was confirmed that end members $CaTiO_3$ and LNT materials had orthorhombic (Pbnm 62) and tetragonal (P4-b2) structures, respectively, as reported previously.[9,10] It can also be seen (Fig. 2) that the orthorhombic structure is maintained for all compositions where x is greater than 0.2. The indexing of CT and 0.2CT-0.8LNT (Fig. 2) is based upon an orthorhombic structure. The data show that 0.2CT-0.8LNT has in-phase, anti-phase tilting ($a^+ b^- b^-$) and A-site ion displacement according to Glazers classification[9] (Peaks 013 & 213 indicate in-phase tilting, 311, 115 & 113 indicate anti-phase tilting and peaks 021 & 210 indicate cation displacement). The composition where the structure changes from orthorhombic (Pbnm 62) to tetragonal (P4-b2) lies between LNT and 0.2CT-0.8LNT; this transition from orthorhombic to the tetragonal structure results in a change from a three tilt system to a one tilt system which is manifested in the disappearance of specific peaks. Examples are the 210 peak which indicates cation displacement. Using Glazers classification, LNT has only anti-phase tilting ($a^0a^0c^-$) indicated by the 133 peak (Fig. 2). The lattice parameters for $CaTiO_3$ to 0.2CT-0.8LNT were a=5.426 Å, b=5.395 Å and c=7.595 Å, whilst for LNT a=b=7.6280 Å c=7.6098 Å.

Figs. 3-7 show backscattered images of the microstructure of xCT-(1-x)LNT series from pure $CaTiO_3$ to $Li_{0.5}Nd_{0.5}TiO_3$. Fig. 3 shows that the microstructure of $CaTiO_3$ (sintered at 1500°C for 5 h) is highly twinned; the grains have uniform shape with average size of 3.5 μm. There are a number of lamella type twins (e.g. B in Fig. 3) indicating the presence of {110} {112} and $[001]_{90}$ type twinning and needle shaped twins (e.g. A in Fig. 3) indicating that during processing, after the initial twinning develops the lamella twins

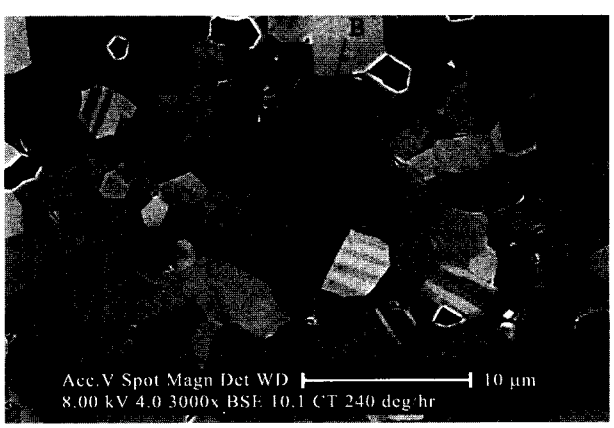

Fig. 3. Electron backscattered image of $CaTiO_3$ sintered at 1500°C: **A** Needle like twins; **B** Lamella type twins, and **C** twins intersecting at 90°.

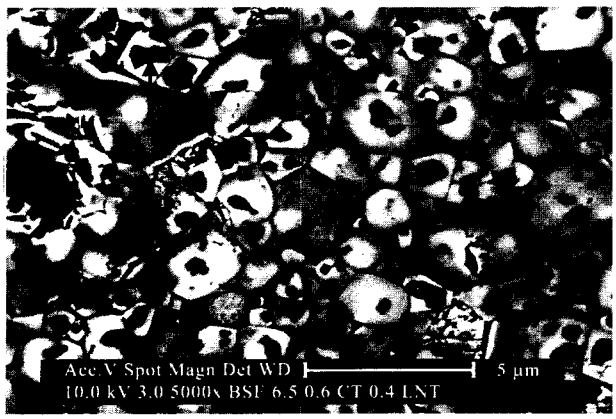

Fig. 4. Electron backscattered image of 0.6CT-0.4LNT; **D** Calcium rich region.

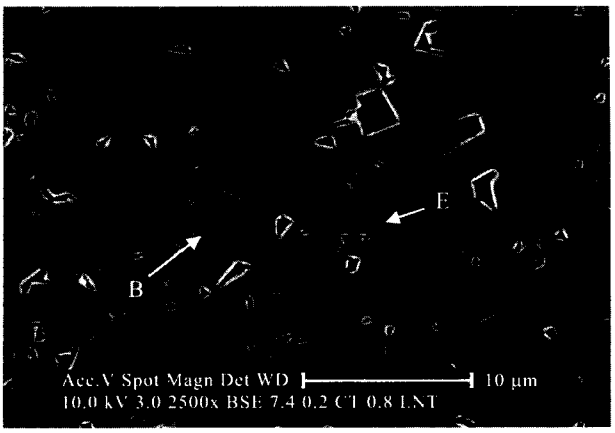

Fig. 6. Electron backscattered image of 0.2CT-0.8LNT: **B** Lamella twinning; **E** boundary rich in Li.

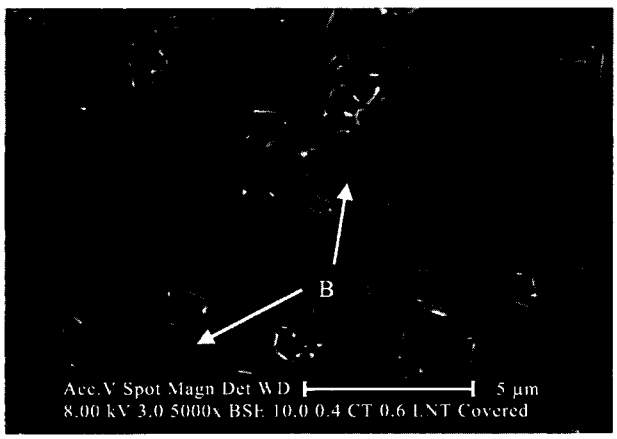

Fig. 5. Electron backscattered image of 0.4CT-0.6LNT; **B** Lamella type twins.

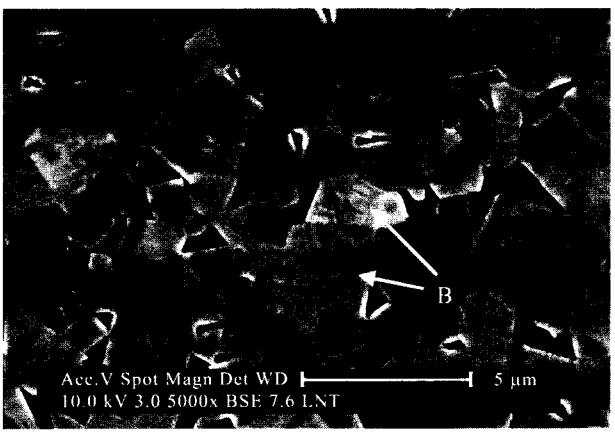

Fig. 7. Electron backscattered image of LNT, indicating the presence of twinning (**B**).

undergo healing and form needle like twins.[10] In addition there are a number of twins that intercept at an angle of 90°, which indicate the presence of {110} and $[001]_{90}$ type twinning (e.g. C in Fig. 3).

As x decreases from 1 to 0.4 in the system xCT-(1-x)LNT, the average grain size decreases significantly from 3.5 μm to 1.3 μm. This decrease is directly linked to the decrease in the sintering temperature from 1500°C for pure $CaTiO_3$ to 1300°C for 0.4CT-0.6LNT. In comparison, in 0.6CT-0.4LNT and 0.4CT-0.6LNT the microstructures are characterised by a number of dark regions, within the grains, which are rich in calcium. The latter may be the result of inhomogeneous powder mixing, but is only visible under backscatter electron images. Decreasing the amount of $CaTiO_3$ further to the composition 0.2CT-0.6LNT results in a uniform microstructure in which there is only a small number of calcium rich regions (Fig. 6). In 0.2CT-0.8LNT (Fig. 6) there is a strong suggestion of Li concentration at the grain edges, as evidenced by the light coloured regions around the grain boundaries. Finally in $Li_{0.5}Nd_{0.5}TiO_3$, the microstructure is characterised by highly rectangular grains 2–5 μm in size (Fig. 7). Although there is no change in the sintering temperature from 0.2CT-0.8LNT to LNT, the increase in grain size can be attributed to the increased lithium in the structure. Figs. 3-7 confirm the presence of twinning in xCT-(1-x) LNT, which is most clearly seen in $CaTiO_3$. The morphology of the twins in Figs. 3-5 is very similar to that observed previously using TEM.[11,12] In Fig. 3 there are a number of grains in which there is cross-hatched morphology, indicating that the {110} and $[001]_{90}$ type twins formed together.[11,12]

Further analysis of the twinning phenomena in xCT-(1-x) LNT is shown in Figs. 8 and 9. Twins form due to microstructural strain within the grains when the structure changes. In the case of $CaTiO_3$, the crystal structure changes from cubic to tetragonal to orthorhombic at 1350°C and 1250°C, respectively. When the crystal lattice twins, the orientation of the grain either side of the twin boundary changes through a specific angle, which is dependent upon the type of twin formed. Fig. 8 shows an EBSD orientation contrast map for $CaTiO_3$. The twins are well defined and show a similar structure to that observed in the backscattered image (Fig. 3). Fig. 9 shows an EBSD orientation contrast map for 0.8CT-0.2LNT. Again the presence of

Fig. 8. EBSD orientation contrast map of $CaTiO_3$.

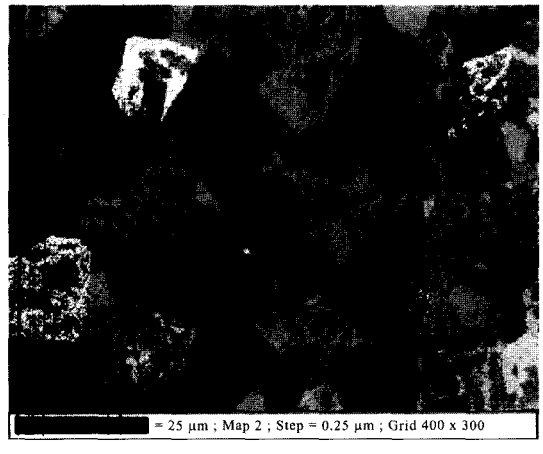

Fig. 9. EBSD orientation contrast map of 0.8CT-0.2LNT.

twinning in the microstructure can be seen, but the definition is not as good, perhaps due to the smaller grain size and higher surface strain. It was noted that the quality of the orientation maps decreases as the LNT content increased; this may be due to structural changes which result in poor matching of the diffraction patterns to the data in the software library. However, EBSD is valuable for distinguishing twins in the microstructure and further developments in the software used for EBSD analysis will enable more detailed analysis of twinning.

Fig. 10 shows the relative permittivity and Q.f. as a function of xCT-1-xLNT. The data for $CaTiO_3$ and LNT compare quite well with published literature.[3,4,6] As the composition changes from $CaTiO_3$ to LNT the relative permittivity decreases from 170 to 80, and the Q.f. decreases from 3800 to 2100 at 2.1 GHz as expected. The changes in relative permittivity and Q.f. with xCT-1-xLNT are the same as for the $xCaTiO_3$-$(1-x)Li_{0.5}Sm_{0.5}TiO_3$ system.[3] However the relative permittivity for xCT-1-xLNT is higher than $xCaTiO_3$-$(1-x)Li_{0.5}Sm_{0.5}TiO_3$ as is predicted by Takahashi *et al.*[6] When Sm is replaced by Nd. Fig. 11 shows τ_f as a function of xCT-1-xLNT. The τ_f for end members $CaTiO_3$ and LNT are 744 to 280 ppm/°C, respectively, in agreement with literature.[3,13]

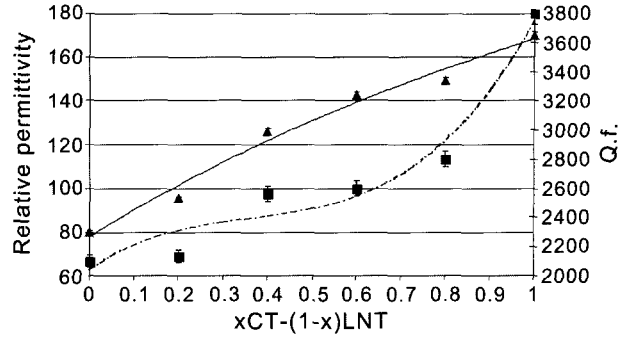

Fig. 10. The relative permittivity (▲) and Q.f. (■) at 2 GHz as a function of composition xCT-(1-x)LNT.

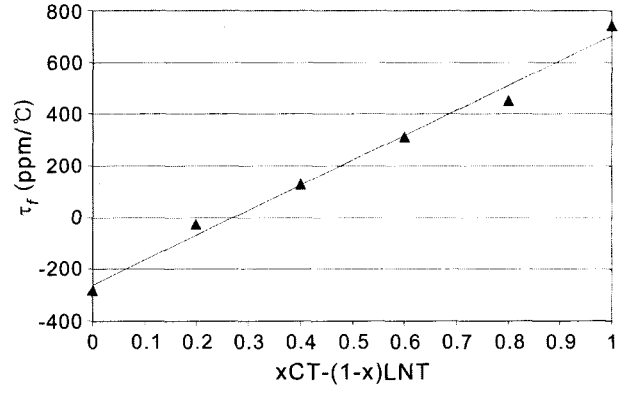

Fig. 11. τ_f (ppm/°C ±2.0%) at 2 GHz as a function of composition xCT-(1-x)LNT.

As the amount of $CaTiO_3$ in xCT-1-xLNT increases, the temperature coefficient of resonant frequency (τ_f) increases linearly. The composition resulting in zero τ_f lies between 0.2CT-0.8LNT and 0.4CT-0.6LNT. The trend for τ_f with composition in xCT-1-xLNT is the same as for the $xCaTiO_3$-$(1-x)Li_{0.5}Sm_{0.5}TiO_3$ system.[3]

4. Conclusions

Ceramics in the system $xCaTiO_3$-$(1-x)Li_{0.5}Nd_{0.5}TiO_3$ for $(0.2 \leq x \leq 1)$ exhibit an orthorhombic (Pbnm No : 62) structure, which is unaffected by the substitution of LNT. SEM backscattered and EBSD analysis of $xCaTiO_3$-$(1-x)Li_{0.5}Nd_{0.5}TiO_3$ showed that the microstructures were highly twinned. The relative permittivity decreases linearly from 170 to 80 as LNT was added to $CaTiO_3$. At the same time Q.f. changes from 3800 to 2000. The addition of LNT to $CaTiO_3$ reduces τ_f linearly from 744 ppm/°C to 240 ppm/°C (end member LNT). Material with zero τ_f material will be achieved between 0.2CT-0.8LNT and 0.4CT-0.6LNT.

Acknowledgment

The support of EPSRC through grant GR/R72655 and provision postgraduate training award to T. Lowe is gratefully acknowledged. We are also grateful for the help and support of Filtronic Comtek.

REFERENCES

1. R. Ubic, I. M. Reaney, and W. E. Lee, "Microwave Dielectric Solid-solution Phase in System BaO-Ln_2O_3-TiO_2 (Ln=Lanthanide Cation)," *Int. Mater. Rev.*, **43** 205-19 (1998).
2. W. S. Kim and K. H. Yoon, "Microwave Dielectric Properties and Far-infrared Reflectivity Characteristics of the $CaTiO_3$-$Li_{0.5-3x}Sm_{0.5+x}TiO_3$ Ceramics," *J. Am. Ceram. Soc.*, **83** [9] 2327-29 (2000).
3. W. S. Kim, K. H. Yoon, and E. S. Kim, "Far-infrared Reflectivity Spectra of $CaTiO_3$-$Li_{0.5}Sm_{0.5}TiO_3$ Microwave Dielectrics," *Mater. Res. Bull.*, **34** 2309-17 (1999).
4. K. H. Yoon, Y. Chang, W. S. Kim, J. B. Kim, and E. S. Kim, "Dielectric Properties of $Ca_{1-x}Sm_{2x/3}TiO_3$-$Li_{0.5}Sm_{0.5}TiO_3$ Ceramics," *Jpn. J. Appl. Phys.*, **35** 5145-49 (1996).
5. J.-S. Kim, C.-I. Cheon, H.-J. Kang, C.-H. Lee, K.-Y. Kim, S. Nam, and J.-D. Byun, "Crystal Structure and Microwave Dielectric Properties of $CaTiO_3$-$(Li_{0.5}Sm_{0.5})TiO_3$-$(Ln_{1/3}Nd_{1/3})TiO_3$ (Ln=La, Dy) Ceramics," *Jpn. J. Appl. Phys.*, **38** 5633-37 (1999).
6. H. Takashi, Y. Baba, K. Ezaki, and K. Shibata, "Microwave Dielectric Properties and Crystal Structure of CaO-Li_2O-(1-x) Sm_2O_2-xLn_2O_3-TiO_2 (Ln : Lanthanide) Ceramic System," *Jpn. J. Appl. Phys.*, **35** 5069-73 (1996).
7. J. Petzelt and N. Setter, "Far Infrared Spectroscopy and Origin of Microwave Losses in Low-loss Ceramics," *Ferroelectrics*, **150** 89-102 (1993).
8. B. Hakki and P. Coleman, "A Dielectric Resonator Method of Measuring Inductive Capacities in the Millimeter Range," *IRE Trans. On Microwave Theory & Techniques*, **MTT-8** 402-10 (1960).
9. A. Glazer, "Simple Ways of Determining Perovskite Structures," *Acta Cryst.*, **A31** 756-62 (1975).
10. E. K. Salje, *et al.*, "Needle Twins and Right-angled Twins in Minerals: Comparison Between Experimental and Theory," *Am. Minerals.*, **83** 811-22 (1998).
11. Y. Wang and C. Liebermann, "Electron Microscopy Study of Domain Structure due to Phase Transitions in Natural Perovskite," *Phys. Chem. of Minerals.*, **20** 147-58 (1993).
12. Y. Wang and C. Liebermann, "Twinning in $MgSiO_3$ Perovskite," *Science*, **248** [4954] 468-71 (1990).
13. H. Takashi, Y. Baba, K. Ezaki, Y. Okamoto, K. Shibata, K. Kuroki, and S. Nakano, "Dielectric Characteristics of $(A_{1/2}^{1+}A_{1/2}^{3+})TiO_3$ Ceramics at Microwave Frequencies," *Jpn. J. of Appl. Phys.*, **30** [9B] 2339-42 (1991).